Available online at www.sciencedirect.com
SCIENCE DIRECT®
Journal of Magnetic Resonance 165 (2003) 9–17
JMR Journal of Magnetic Resonance
www.elsevier.com/locate/jmr

Parameter maps of ^{1}H residual dipolar couplings in tendon under mechanical load

R. Fechete, D.E. Demco, and B. Blümich*

Institut für Technische Chemie und Makromolekulare Chemie, Rheinisch-Westfälische Technische Hochschule, Worringerweg 1, Aachen D-52056, Germany

Received 8 April 2003; revised 30 July 2003

Abstract

Proton multipolar spin states associated with dipolar encoded longitudinal magnetization (DELM) and double-quantum (DQ) coherences of bound water are investigated for bovine and sheep Achilles tendon under mechanical load. DELM decay curves and DQ buildup and decay curves reveal changes of the ^{1}H residual dipolar couplings for tendon at rest and under local compression forces. The multipolar spin states are used to design dipolar contrast filters for NMR ^{1}H images of heterogeneous tendon. Heterogeneities in tendon samples were artificially generated by local compression parallel and perpendicular to the tendon plug axis. Quotient images obtained from DQ-filtered images by matched and mismatched excitation/reconversion periods are encoded only by the residual dipolar couplings. Semi-quantitative parameter maps of the residual dipolar couplings of bound water were obtained from these quotient images using a reference elastomer sample. This method can be used to quantify NMR imaging of injured ordered tissues.

Keywords: NMR parameter images of residual dipolar couplings; ^{1}H double-quantum-filtered NMR images; Dipolar encoded longitudinal magnetization; Tendon

1. Introduction

Most biological tissues like tendon, cartilage, kidney, muscle, white matter, and optic nerves possess some degree of order. In such ordered tissues, where the molecular motion of some constituents is anisotropic, dipolar, and quadrupolar interactions of nuclear spins are not averaged to zero. In such cases homonuclear and heteronuclear multiple-quantum (MQ) NMR coherences [1–3] can be formed. These coherences give information about the effect of the anisotropic motion of the water molecules and sodium ions in intact biological tissues (for a review, see [3]). In collagen-containing tissues such as tendon, ligaments, cartilage, skin, blood vessels, and nerves double-quantum (DQ) coherences are formed as a result of the water interaction with the collagen fibers. The tightly bound water molecules that penetrate the triple-helix interstices are fixed by two hydrogen bonds. These water molecules can rotate about the axis defined by the two bonds reducing the dipolar proton–proton interaction along the rotation axis. A similar anisotropy produced by preaveraging of spin interactions along the end-to-end vector [4] can be measured by the ^{1}H residual dipolar couplings of the side-chain of the macromolecules in another class of soft solids that is represented by the synthetic elastomers [5–8] (and references therein).

The presence of residual dipolar couplings allows MQ coherences to be generated in ordered tissues [3]. These MQ coherences, in particular double-quantum (DQ) coherences, have the advantage to suppress the intense signal of free water and to a high degree the signals originating from the macromolecules. Therefore, the observation of MQ coherences represents a convenient approach to investigate local and macroscopic order in a variety of tissues.

Recently, ^{1}H and ^{2}H DQ-filtered (DQF) magnetic resonance imaging (MRI) has been applied for visualization of ordered tissues. Deuteron DQF-MRI was

* Corresponding author. Fax: +49-241-8888-185.
E-mail address: bluemich@mc.rwth-aachen.de (B. Blümich).

1090-7807/$ - see front matter © 2003 Elsevier Inc. All rights reserved.
doi:10.1016/S1090-7807(03)00278-7

reported for bovine nasal cartilage [9], the sciatic nerve of a rat [10], and rat blood vessels [11]. However, ^{2}H NMR poses disadvantages compared to ^{1}H NMR for in vivo MRI because of a low gyromagnetic ratio and a low concentration in biological tissues. Proton images of various ordered tissues have been also reported [3,12,13]. In vivo ^{1}H DQF-MRI was performed on human wrist and ankle [12]. The same method was applied to joint tissues of rabbits for selective visualization of tendon, meniscus, and articular cartilage [13].

Multiple-quantum coherences, especially double-quantum coherences of ^{1}H in dipolar-coupled systems, have been explored recently for measurements of residual dipolar couplings in elastomers like poly(styrene-co-butadiene) [14], synthetic poly(isoprene) [6], and natural rubber [8]. Proton residual dipolar couplings of elastomers chains were used to generate contrast in NMR images [15] of samples with distributions of cross-link density and stress in stretched elastomers [16,17]. Dipolar contrast filters are discussed on the basis of dipolar encoded longitudinal magnetization (DELM) as well as DQ and triple-quantum coherences. Two-dimensional maps of stress distributions were presented for a strained natural rubber band with a cut on one side measured with DELM and DQ filters [17].

The goal of this paper is to investigate the intriguing possibility to obtain ^{1}H NMR images of tendon encoded by the residual dipolar couplings of bound water especially under mechanical load conditions. Dipolar filters based on DELM and DQ coherences are used for this purpose. A combination of matched and mismatched pulse sequences used for the excitation of DQ coherences can be used for obtaining maps of residual dipolar couplings. The local compression forces acting along different directions of a tendon plug enhance the heterogeneity in tendon samples and mimic the effect of injuries.

2. Experimental

2.1. Materials

Samples of Achilles tendon from sheep and cattle were kept at -18 °C after excision until their measurement at room temperature 20 ± 1 °C. A plug was cut from the middle of the tendon and was wrapped with teflon tape in order to avoid dehydration. A new tendon plug was used after about 12 h of measurements to preclude tissue degradation. The tendon plugs were not immersed in any susceptibility matching liquid.

2.2. NMR experiments

The NMR experiments were performed at a ^{1}H frequency of 299.87 MHz on a Bruker DMX-300 spectrometer. DELM decay curves and DQ build-up curves were recorded with the five-pulse sequence [18,19] (cf. Figs. 1a and b) with matched excitation/reconversion periods. DQ decay curves are measured using mismatched creation/reconversion periods [20] (cf. Figs. 1a and b). The phase cycling schemes are described in [16–20]. A 15 μs 90° pulse, and a 1 s recycle delays were used. The evolution time and the z-filter delay were fixed to $t_1 = 20$ and $\tau_f = 5$ μs, respectively.

For two-dimensional (2D) images and parameter maps a phase-and-frequency encoding procedure was employed [15]. The dipolar filters based on multipolar spin states in combination with MRI were implemented following the pulse sequence shown in Figs. 1c and d. The micro-imaging unit included a home-built gradient coil system. In all images the spatial resolution was about 300 μm in both directions with a field of view of about $(20\,\text{mm})^2$. The maximum achievable gradient strength was approximately 93 mT/m. The gradient was stepped through 64 gradient values. The total duration for acquisition of 2D filtered images was on the order of

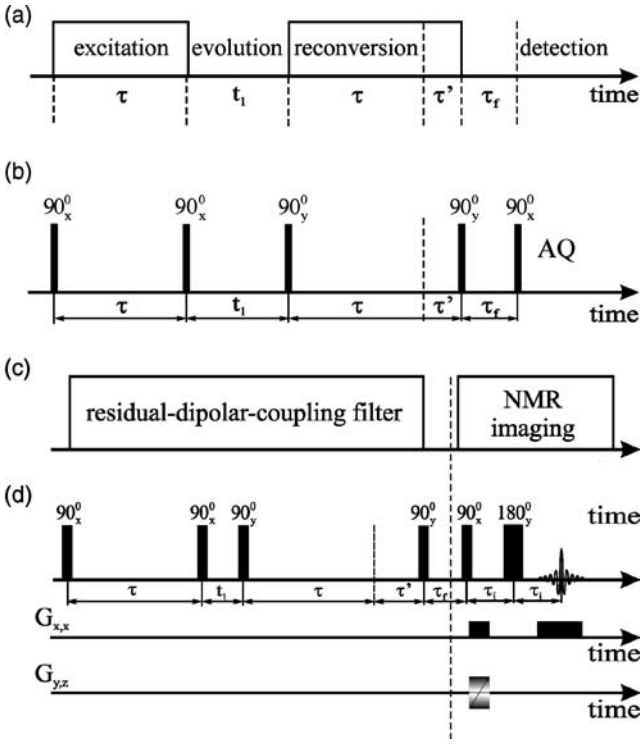

Fig. 1. (a) General scheme used for measurement of multiple-quantum-filtered spectra. (b) The five-pulse sequence used for measuring double-quantum buildup curves and dipolar-encoded longitudinal magnetization. The multiple-quantum (MQ) excitation, evolution, reconversion, z-filter, and detection periods are denoted by τ, t_1, τ, τ_f, and t_2, respectively. The mismatch time between excitation and reconversion is τ'. In the case of matched excitation and reconversion $\tau' = 0$. (c) General scheme for recording images weighted by residual dipolar couplings. (d) Four pulse sequence for multipolar spin states filtering according to residual dipolar couplings followed by a z-filter and space encoding by 2D spin–echo imaging.

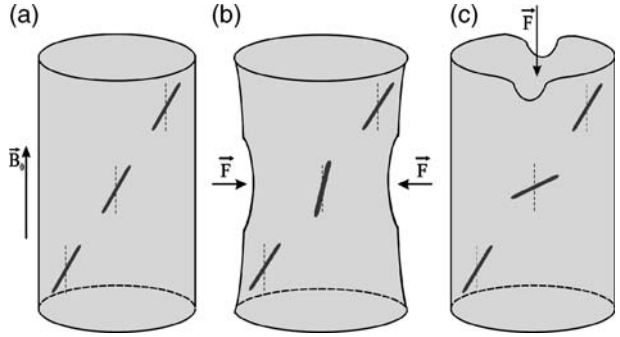

Fig. 2. Pictorial representation of the local changes in the collagen fibril orientation due to the compression forces ($\vec{F}$). The tendon plug axis is oriented parallel with the direction of the static magnetic field $\vec{B}_0$ The black sticks mimics parts of the collagen fibrils and the angle between the fibrils and the tendon plug axis shows the existence of an angular distribution [3,21]. (a) The angular distribution of the collagen fibrils is approximately uniform in the tendon at rest. (b) Under radial compression the main effect is the reduction of the width of the orientation distribution function in the compressed region. (c) In the presence of the local axial compression mainly the center of the angular distribution is shifted away form the tendon plug axis.

3 h. The 90° and 180° pulse lengths for image acquisitions were 20 and 47 μs, respectively. Recycle delays of 1 s were used in all experiments. The evolution times for measuring LM decays, DQ build-up, and DQ decay intensities were fixed to $t_1 = 10\,\mu s$. In all experiments, the excitation and reconversion times were set to $\tau = 200\,\mu s$ and $\tau' = 40\,\mu s$. For 2D spin–echo images [15] the echo time was $\tau_i = 0.85$ ms. At the beginning of each experiment the tendon plug axis was adjusted parallel to the direction of the static magnetic field. At this orientation the ^{1}H residual dipolar coupling of bound water is at its maximum [3,21].

For the experiments performed with sheep tendon a teflon rope was wound around the tendon plug in the central region on 8 mm length producing a local compression perpendicular to the plug axis (see Fig. 2b). The compression ratio was about $\lambda \approx 0.8$. The plug axis is parallel with the axis of the tendon and the direction of the static magnetic field (Fig. 2a). A special device was build for applying uniform and local compression forces along the plug axis. The bovine tendon samples were placed in a glass tube and a teflon rod was pressed on the plug along the tube axis by a screw (see Fig. 2c). For imaging experiments, the face of the teflon rod in contact with the tendon plug had an elevated riffle with the dimensions $1\,mm \times 10\,mm$ along its diameter. The compression ratio produced by this part on the central region of the tendon was about $\lambda \approx 0.7$.

3. Theory

For tendon, the ^{1}H NMR signal originates from free water, bound water, and collagen fibrils. In the following, we discuss only the bound water signal, which can be easily detected and separated from the free water and protein signals [3] (and references therein). The existence of dipolar splitting in ^{1}H DQ-filtered spectra [1–3,21] shows that the protons of the water molecules can be considered in a good approximation to be a quasi-isolated spin-pair. This approximation is valid only for short times when spin diffusion to the collagen protons can be neglected. Moreover, the dipolar coupling between spin pairs is averaged on the time scale of the NMR experiment which results from the reorientation motion of the bound water as well as from the chemical exchange between free and bound water molecules [1–3]. As a result of this partial motional averaging the axis of the dipolar tensor is oriented on average along the collagen-fibril direction, which defines the local director having the angle β with the direction of $\vec{B}_0$ and the angle $\tilde{\beta}$ with the axis of symmetry of the tendon plug. It is assumed that the distribution of collagen fibrils around the tendon axis is uniaxial, so that the orientation distribution can be specified in terms of a single angular variable $\tilde{\beta}$. The averaged Hamiltonian of the spin pair is given by

$$\bar{H}_d = \left(-\sqrt{\frac{3}{2}} \right) DSP_2(\cos\beta) T_{2,0}, \tag{1}$$

where D is the dipolar coupling constant, S is the dynamic order parameter [5], $P_2(\cos\beta)$ is the second order Legendre polynomial, and $T_{2,0}$ is an irreducible tensor operator defined, for instance, in [6]. To simplify the notation, Eq. (1) is rewritten as

$$\bar{H}_d = \varpi_d T_{2,0}, \tag{2}$$

where ϖ_d is the residual dipolar coupling, which includes the angular anisotropy. The effect of slow hydrogen exchange can be considered to be present in the value of the dynamic order parameter [21].

The spin system response to the five-pulse sequence used for excitation of multipolar spin states (cf. Fig. 1) can easily be evaluated in the density operator formalism [3,6]. For the case of an isolated spin-1/2 pair only dipolar encoded longitudinal magnetization and DQ coherences can be excited and separated by phase cycling [6,16,17].

3.1. Dipolar encoded longitudinal magnetization decay curve

In the case of spin-1/2 pairs, the evolution of longitudinal magnetization in the five-pulse sequence versus τ is dipolar encoded [6]. The DELM signal is given by

$$S_{\mathrm{DELM}}(\tau) \propto \left\langle \cos^2\left(\sqrt{\frac{3}{2}} \varpi_d \tau \right) \exp\left(-\frac{2\tau}{T_{2,\mathrm{eff}}} \right) \right\rangle, \tag{3}$$

where the effective decay time of the SQ during the excitation and reconversion periods is $T_{2,\mathrm{eff}}$. This quantity

is also orientation dependent [3]. The average of ϖ_d and of $T_{2,\mathrm{eff}}$ over the orientation of collagen fibers is denoted by $\langle(\cdots)\rangle$.

For short dipolar-encoding times, i.e., for $\varpi_d\tau \ll 1$, and $2\tau \ll T_2^*$, Eq. (3) becomes

$$S_{\mathrm{DELM}}(\tau) \propto 1 - \frac{3}{4}\langle\varpi_d^2\rangle^2\tau^2. \tag{4}$$

This relationship shows that the intensity of the filtered signal is decaying with an initial slope related to the residual dipolar couplings.

3.2. Double-quantum buildup curve

The DQ buildup curves can be measured using the pulse sequence of Fig. 1 with the mismatch parameter $\tau' = 0$ and variable τ. The DQ signal is given by [6]

$$S_{\mathrm{DQ}}(\tau) \propto \left\langle \sin^2\left(\sqrt{\frac{3}{2}}\varpi_d\tau\right)\exp\left(-\frac{2\tau}{T_{2,\mathrm{eff}}}\right)\right\rangle. \tag{5}$$

In a good approximation, Eq. (5) can be rewritten as

$$S_{\mathrm{DQ}}(\tau) \propto \left\langle \sin^2\left(\sqrt{\frac{3}{2}}\varpi_d\tau\right)\right\rangle \exp\left(-\frac{2\tau}{\bar{T}_{2,\mathrm{eff}}}\right), \tag{6}$$

where $\bar{T}_{2,\mathrm{eff}}$ is the orientation-averaged effective transverse relaxation time.

The DQ buildup curve described by Eq. (6) can be easily evaluated in the initial DQ excitation/reconversion regime, i.e., for $\varpi_d\tau \ll 1$ and $2\tau \ll T_2^*$. We finally get

$$S_{\mathrm{DQ}}(\tau) \propto \frac{3}{2}\langle\varpi_d^2\rangle\tau^2 + \cdots. \tag{7}$$

The above equation can also be obtained if the proton exchange is taken explicitly into account during excitation and reconversion of DQ coherences in the limit of very slow proton exchange, i.e. for $k \ll \langle\varpi_d^2\rangle^{1/2}$, where k is the sum of the forward and backward proton exchange rates [3,21].

3.3. Double-quantum decay curve

For $\tau' > 0$, the spin system response of an isolated spin-1/2 pair to the pulse sequence of Fig. 1 was discussed in [20]. The DQ-filtered signal is given by

$$S_{\mathrm{DQ}}(\tau) \propto \left\langle \sin\left(\sqrt{\frac{3}{2}}\varpi_d(\tau+\tau')\right)\sin\left(\sqrt{\frac{3}{2}}\varpi_d\tau\right)\right\rangle. \tag{8}$$

In the presence of transverse relaxation of single-quantum coherences during excitation and reconversion periods, Eq. (8) has to be multiplied by the function $\exp[-(2\tau+\tau')/\bar{T}_{2,\mathrm{eff}}]$. If the τ' interval fulfills the conditions $\varpi_d\tau' \ll 1$, and $\tau' \ll T_{2,\mathrm{eff}}$ we can write for Eq. (8),

$$S_{\mathrm{DQ}}(\tau') \propto \left\langle \sin^2\left(\sqrt{\frac{3}{2}}\varpi_d\tau\right)\left(1-\frac{3}{4}\varpi_d^2\tau'^2\right)\right\rangle \times \exp\left[-2\tau/\bar{T}_{2,\mathrm{eff}}\right]. \tag{9}$$

This equation is derived for a parameter τ with a value in the region of the maximum of the DQ buildup curve, i.e., for

$$\left\langle \sin^2\left(\sqrt{\frac{3}{2}}\varpi_d\tau\right)\right\rangle \approx 1$$

and

$$\left\langle \cos\left(\sqrt{\frac{3}{2}}\varpi_d\tau\right)\right\rangle \approx 0.$$

If these conditions are fulfilled then Eq. (9) can be approximated by

$$S_{\mathrm{DQ}}(\tau') \propto \left\langle \sin^2\left(\sqrt{\frac{3}{2}}\varpi_d\tau\right)\right\rangle\left(1-\frac{3}{4}\langle\varpi_d^2\rangle\tau'^2\right) \times \exp\left[-2\tau/\bar{T}_{2,\mathrm{eff}}\right]. \tag{10}$$

It was shown that the approximations involved in the derivation of Eq. (10) are valid for elastomers [20] and we can expect then to be fulfilled also for the bound water in ordered tissues. Finally, the normalized DQ-filtered signal is given by

$$\frac{S_{\mathrm{DQ}}(\tau')}{S_{\mathrm{DQ}}(\tau)} \approx \left\langle\left(1-\frac{3}{4}\langle\varpi_d^2\rangle\tau'^2\right)\right\rangle, \tag{11}$$

i.e., the signal represents a DQ *decay curve* where the initial amplitude $S_{\mathrm{DQ}}(\tau)$ is given by the DQ-filtered signal obtained from the matched excitation/reconversion of duration τ.

3.4. Residual dipolar coupling parameter maps

Let us consider in the following a NMR image obtained using a matched DQ dipolar filter (cf. Fig. 1). The filtered signal from the voxel specified by the vector of position $\vec{r}$ is given by

$$S_{\mathrm{DQ}}(\tau;\vec{r}) \propto \rho(\vec{r})\left\langle \sin^2\left(\sqrt{\frac{3}{2}}\varpi_d(\vec{r})\tau\right)\right\rangle \times \exp\left[-2\tau/\bar{T}_{2,\mathrm{eff}}(\vec{r})\right], \tag{12}$$

where $\rho(\vec{r})$ is the spin density and the residual dipolar couplings as well as the effective transverse relaxation time are distributed in space.

For an image obtained by a mismatched DQ dipolar filter the signal from a voxel can be written from Eq. (10) as

$$S_{\mathrm{DQ}}(\tau';\vec{r}) \propto \rho(\vec{r})\left\langle \sin^2\left(\sqrt{\frac{3}{2}}\varpi_d\left(\vec{\mathrm{r}}\right)\tau\right)\right\rangle \times \left(1-\frac{3}{4}\left\langle \varpi_d^2\left(\vec{\mathrm{r}}\right)\right\rangle \tau'^2\right)\exp\left[-2\tau/\bar{T}_{2,\mathrm{eff}}\left(\vec{r}\right)\right]. \quad (13)$$

We can define a *ratio-difference image* from Eqs. (12) and (13)

$$\frac{S_{\mathrm{DQ}}\left(\tau;\vec{r}\right)}{S_{\mathrm{DQ}}\left(\tau';\vec{r}\right)} - 1 \approx \frac{3}{4}\left\langle \varpi_d^2(\vec{r})\right\rangle \tau'^2. \quad (14)$$

This is a *residual dipolar coupling parameter map* if the constant factors are taken into account. A semi-quantitative map of residual dipolar couplings can be also generated if a homogeneous reference sample with similar properties is simultaneously imaged. This map is described by

$$\left\langle \varpi_d^2(\vec{r})\right\rangle^{1/2} \approx \left(\left(\frac{S_{DQ}\left(\tau;\vec{r}\right)}{S_{DQ}\left(\tau';\vec{r}\right)}-1\right)\Big/\left(\frac{S_{DQ}(\tau)_{\mathrm{ref}}}{S_{DQ}(\tau')_{\mathrm{ref}}}-1\right)\right) \times \left\langle \varpi_d^2\right\rangle_{\mathrm{ref}}^{1/2}. \quad (15)$$

The reference residual dipolar coupling $\langle \varpi_d^2\rangle_{\mathrm{ref}}^{1/2}$ has to be measured in a separate experiment using for instance DQ buildup or decay curves [6,16,17].

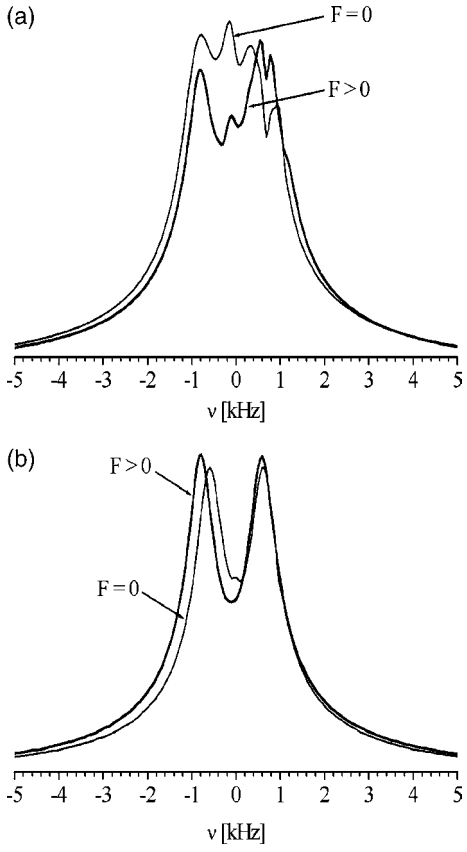

Fig. 3. Proton NMR spectra of bound water in sheep Achilles tendon obtained after a 90° pulse (a) and after DQ filtration (b). A radial compression force (F) was applied on the tendon plug. Two different spectra are shown for $F = 0$ and $F > 0$.

4. Results and discussions

4.1. Proton DQ-filtered spectra of bound water in tendon at rest and under compression

The effect of a radial compression with force (F) on the cylindrical surface of the sheep tendon plug is illustrated in Fig. 3a by ^{1}H NMR spectra measured with single-pulse excitation. If the spectrum for $F > 0$ is compared with that measured for $F = 0$ a small broadening of the spectrum is detected in the presence of radial compression. Moreover, for $F > 0$ the integral intensity of the spectrum is lower (see Fig. 3a), which can be explained by a loss of free water under compression. The spectrum is a superposition of the signals from free water that arises near the origin of the frequency scale, the signal of bound water, and a very broad signal from collagen.

For the same conditions as above ^{1}H DQ-filtered spectra are shown in Fig. 3b. These spectra were measured with the pulse sequence of Fig. 1 for $\tau = 300$, $t_1 = 20$, and $\tau_f = 20\,\mu s$. A dipolar splitting is observed that can be attributed to the bound water [1–3,21] because the signal from free water is suppressed by the DQ filter. Under radial compression the splitting increase, which means that the ^{1}H residual dipolar couplings of the bound water molecules increase due mainly to an increase in the local orientation of the collagen fibrils relative to the direction of the static magnetic field (see below). This interpretation is supported by a study of the orientation dependence of the ^{1}H residual dipolar couplings in sheep tendon [21]. We can conclude that the effect of tendon deformation by the radial compression can be clearly detected by the dipolar splitting of the DQ-filtered signals.

4.2. DELM decay curves, and DQ buildup and decay curves of bound water in tendon with and without compression

DELM and DQ coherences were measured with the pulse sequence of Fig. 1 for Achilles tendon from sheep under radial compression. The decay and buildup curves are shown in Fig. 4. The encoding with residual dipolar couplings is dominant only in the initial time regime of these curves. At later times a supplementary encoding by transverse relaxation time becomes important. In the presence of the compression force the initial slopes of all the curves increase (see Fig. 4). This indicates an increase in the ^{1}H residual dipolar couplings due to a

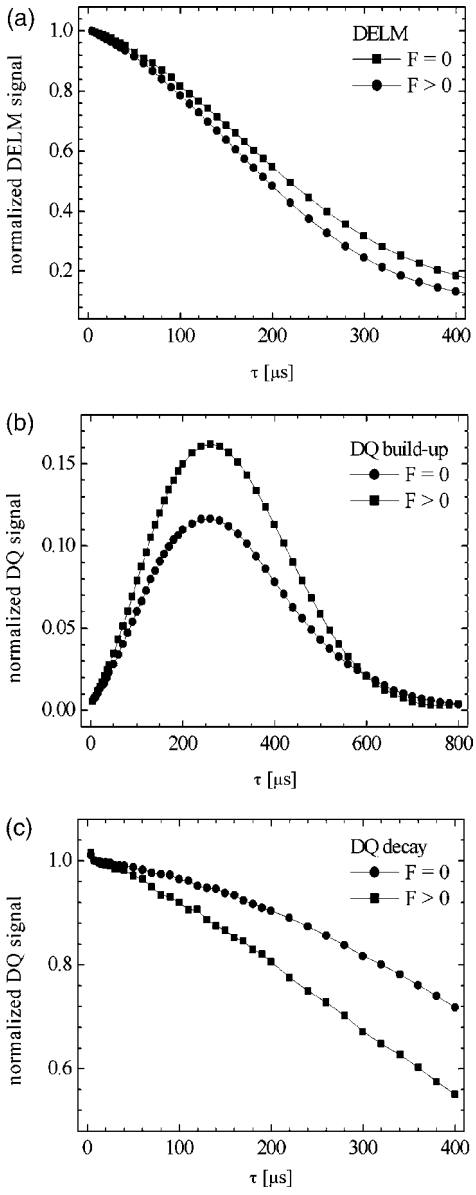

Fig. 4. Evolution of ^{1}H multipolar spin states evolution as a function of the excitation/reconversion period τ for DELM (a), DQ coherences (b), and the mismatch parameter τ' (c) (cf. Fig. 1). All the data are recorded on sheep Achilles tendon at rest ($F = 0$) and under radial compression ($F > 0$).

reduced angular distribution of the collagen fibrils. These curves can be used for selecting the dipolar parameter filters for the NMR images.

Some features of the dipolar filters based on DELM and DQ multipolar spin states can be inferred from the curves in Fig. 4. The highest signal-to noise ratio is obtained by the DELM and the lowest by the DQ buildup curves. Therefore, the resolution of the images is expected to be higher if the first method is used for dipolar filtering. However, the suppression of the free water signal is achieved only by the DQ filter. Moreover, the intense DQ decay curve is superior to the DQ buildup curve in setting the parameters of a residual dipolar filter. The residual dipolar couplings can be quantified without interference from transverse relaxation effects and excitation of high-order quantum coherences only in the regime of short excitation/reconversion times or for small values of the mismatch parameter τ' [20].

4.3. Proton images and residual dipolar coupling parameter maps for tendons under compression

Fig. 5 depicts a comparison of 2D ^{1}H spin–echo images obtained without and with a DELM filter (cf. Fig. 2) for sheep Achilles tendon radially compressed. Both images are encoded by the spin density, transverse relaxation, and residual dipolar couplings, and are affected by the free water signal. Depending on the parameters of the pulse sequences the contrast is expected to be of the same order of magnitude. The advantage of measuring DELM-filtered images is related to the possibility (not shown) to obtain residual dipolar couplings parameter maps in a *model free* way [17]. This is not the case with the images based on the Hahn echo where a

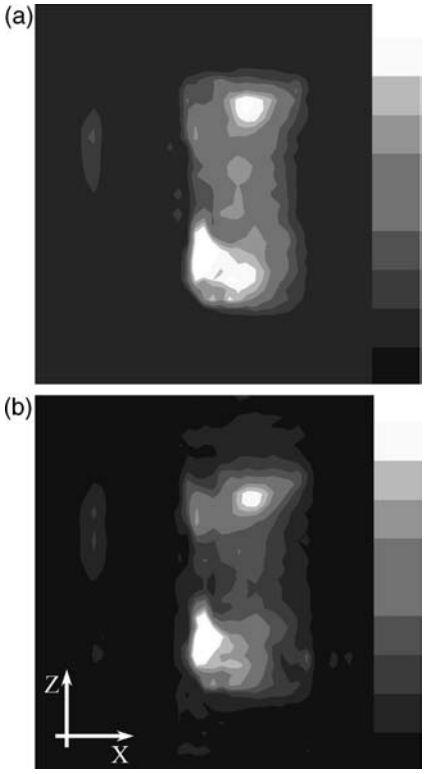

Fig. 5. Proton NMR images of sheep Achilles tendon with radial compression using no filter (a), and a DELM filter (b) (cf. Fig. 1). The tendon plug axis is parallel with the z-direction of the static magnetic field. The length of the plug is 12 mm and the diameter is about 10 mm. Two-dimensional images in the plane (x, z) have been measured without slice selection. On the left hand side of (a) and (b) the images of a reference sample from cross-linked natural rubber are shown.

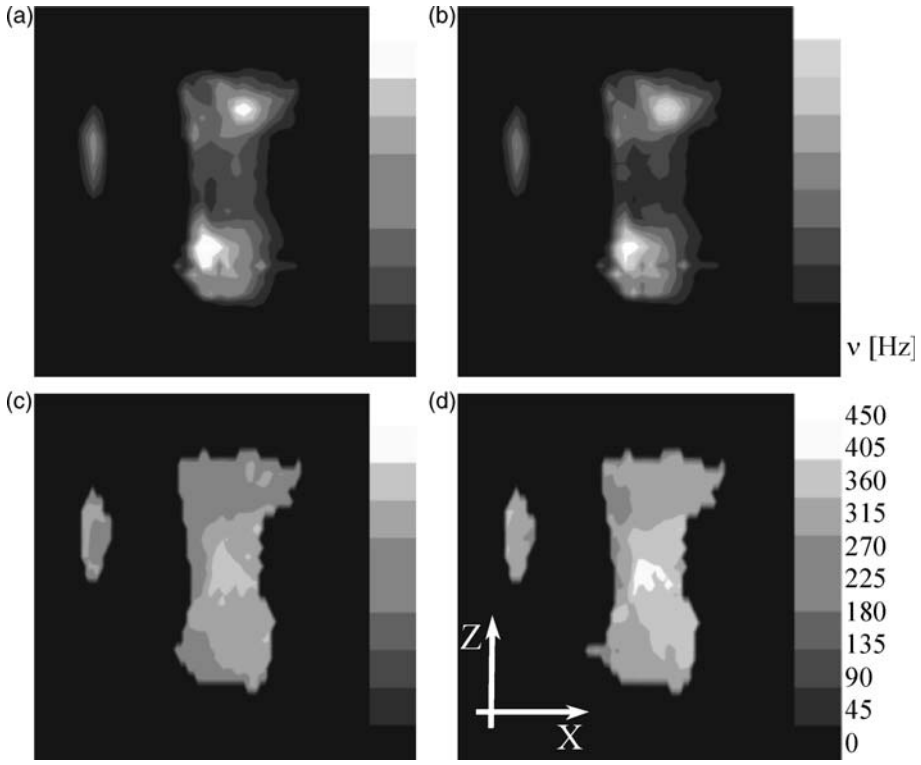

Fig. 6. Proton DQ-filtered images of sheep Achilles tendon with radial compression using the matched (a) and mismatched (b) pulse sequences (cf. Fig. 1). (c) Quotient image of the matched (a) to mismatched (b) DQ-filtered images. (d) Proton residual dipolar coupling map of tendon calibrated with the signal from a cross-linked natural rubber reference sample shown on the left-hand side of (a)–(d) images. The length of the plug is 12 mm and the diameter is about 10 mm. The tendon plug axis is parallel with the z direction of the static magnetic field. Two-dimensional images in the plane (x,z) are shown without slice selection.

complex model is needed of extraction of the information related to the residual dipolar couplings (for a discussion of this topic, see [7]).

The suppression of the free water NMR signal is achieved using DQ dipolar filters. The ^{1}H images and residual dipolar parameter map for the sheep Achilles tendon with radial compression are shown in Fig. 6. A DQ dipolar filter with matched excitation/reconversion periods and $\tau = 200\,\mu s$ is shown in Fig. 6a. The image obtained with the mismatched pulse sequence with $\tau = 200$ and $\tau' = 40\,\mu s$ for the same sample is presented in Fig. 6b. Both images are encoded in a complex manner by the spin density, transverse relaxation, and residual dipolar couplings. If the last effect is dominant the DQ-filtered images will have the highest intensity in the region of the radial compression. This effect is not observed in either image. The strongest signal is detected in the rest regions of the tendon that is due to the migration of the free water in these regions in response to the compression and an increase in the bound water concentration. Fig. 6c shows the quotient of the images from Figs. 6a and b. This image shows clearly a different distribution of the pixel intensities compared to the source images. The highest intensity is present in the deformed region of the tendon. The spin density does not encode the pixels of the quotient image and the effect of the transverse relaxation is also eliminated to a good approximation.

A semi-quantitative residual dipolar-coupling map can be generated from the quotient map of Fig. 6c using Eq. (15). A small piece of crosslinked natural rubber was used as reference sample and its image is shown on the left-hand side in Figs. 6a–d. The ^{1}H residual dipolar coupling of the reference rubber sample was measured in a separate experiment from the DQ buildup curve, and the value estimated based on the procedure discussed in [6] is $(\langle \varpi_d^2 \rangle)^{1/2}/2\pi = 320 \pm 30\,\mathrm{Hz}$.

Similar ^{1}H images and residual dipolar parameter maps were measured for bovine Achilles tendon under compression along the tendon plug axis (cf. Figs. 7 and 8). This force was applied locally along one diameter of the transverse section of the plug. The same reference sample used as before was positioned in the glass tube parallel to the tendon plug. The distribution of the residual dipolar couplings shown in the map of Fig. 8d is different from that of Fig. 6d. Lower values of the residual dipolar couplings are detected in the region of compression (see below).

The effect of the deformation forces applied in the radial directions and along the axis of the tendon detected via changes in the values of the residual dipolar couplings can be understood based on the changes in the collagen

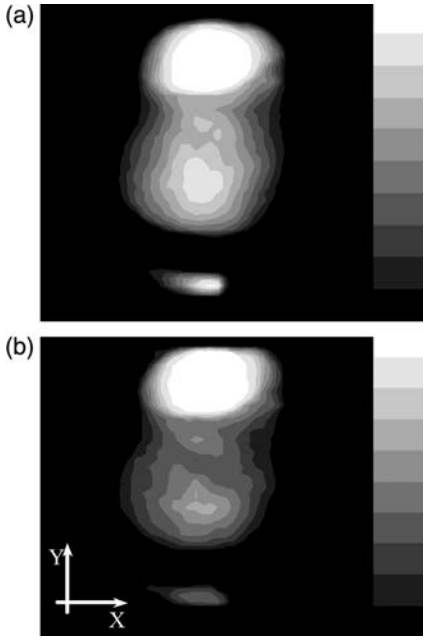

Fig. 7. Proton NMR images of a plug from bovine Achilles tendon compressed along the tendon axis in the central region of the transverse section acquired without (a), and with a DELM filter (b) (cf. Fig. 1). The tendon plug axis is parallel to the z direction of the static magnetic field. The length of the plug is 12 mm and the diameter is about 10 mm. Two-dimensional images in the plane (x, y) are shown without slice selection. On the bottom of (a) and (b) the image of a reference sample from a cross-linked natural rubber is shown.

fibril orientation distribution (see Fig. 2). In tendon, collagen fibrils are not oriented strictly parallel to the tendon axis [3,21]. A uniaxial angular distribution was measured with the center of the distribution tilted away from the plug axis by few degrees (cf. Fig. 2a), and the width of the postulated Gaussian distribution was $19 \pm 1°$ [21]. Under radial compression the main effect is the reduction of the width of the orientation distribution in the compressed region (see Fig. 2b). Moreover, the average orientation direction of the collagen fibrils is than more parallel with the direction of the static magnetic field $\vec{B}_0$. Hence, the values of the residual dipolar couplings of bound water increase in this sample region as shown by the parameter map in Fig. 6d. In the presence of the axial compression forces the center and probably also the width of the orientation distribution are modified compared to those of the tendon regions at rest (see Fig. 2c). The increase in the polar angle of the collagen fibrils relative to $\vec{B}_0$ reduces the value of the residual dipolar couplings in the compressed region (see Fig. 8d).

5. Conclusions

The change in ^{1}H residual dipolar couplings of the bound water in Achilles tendons in response to load was investigated using parameter maps and NMR images.

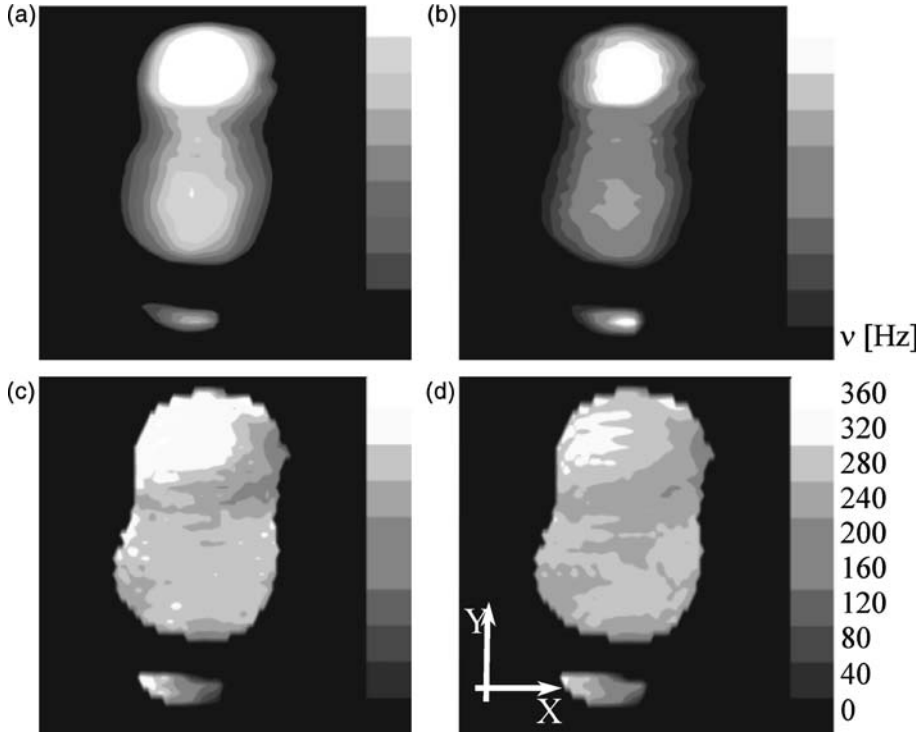

Fig. 8. Proton DQ-filtered images of bovine Achilles tendon compressed along the tendon axis in the central region of the transverse section of the plug using the matched (a), and the mismatched (b) pulse sequences (cf. Fig. 1). Quotient of images (a) and (b) is shown in the image (c). (d) Proton residual dipolar coupling map of tendon calibrated with the signal of a reference sample. The tendon plug axis is parallel with the z direction of the static magnetic field. The length of the plug is 12 mm and the diameter is about 10 mm. Two-dimensional images in the plane (x, y) are shown without slice selection. On the bottom of (a)–(d) the image of a reference sample from crosslinked natural rubber is shown.

Two new methods are presented for recording images of the tendon encoded by the ^{1}H residual dipolar couplings. The first method exploits dipolar encoded longitudinal magnetization and the other one uses the mismatched DQ-filtered signals. The advantage of these methods compared with others based on DQ buildup curves is an increase in the signal-to-noise ratio and hence in the image resolution.

The combination between images measured by matched and mismatched pulse sequences for the excitation of the DQ coherences allows us to obtain the residual dipolar coupling parameter map of the tendon samples. The changes in the residual dipolar couplings under radial and longitudinal compression can be detected with good contrast in the parameter maps and in the images. The use of a reference sample reduces the time needed to acquire residual dipolar coupling maps.

These results open the possibility to use residual dipolar coupling maps to characterize qualitatively and quantitatively injuries and healing of the ordered tissues.

Acknowledgments

This project was supported by the Deutsche Forschungsgemeinschaft (DE 780/1-1) is gratefully acknowledged. The authors are also grateful to Prof. Dr. Gil Navon and Dr. Uzi Eliav for helpful discussions and to Klaus Kupferschläger for building the compression device.

References

[1] U. Eliav, G. Navon, A study of dipolar interactions and dynamic processes of water molecules in tendon by ^{1}H and ^{2}H homonuclear and heteronuclear multiple-quantum-filtered NMR spectroscopy, J. Magn. Reson. 137 (1999) 295–310.
[2] U. Eliav, G. Navon, Multiple quantum filtered NMR studies of the interaction between collagen and water in tendon, J. Am. Chem. Soc. 124 (2002) 3125–3132.
[3] G. Navon, H. Shinar, U. Eliav, Y. Seo, Multiquantum filters and order in tissues, NMR Biomed. 14 (2001) 112–132.
[4] J.-P. Cohen Addad, NMR and fractal properties of polymeric liquids and gels, Prog. NMR Spectrosc. 25 (1993) 1–316.
[5] D.E. Demco, S. Hafner, H.W. Spiess, Multidimensional NMR techniques for the characterization of viscoelastic materials, in: V.M. Litvinov, P.P. De (Eds.), Spectroscopy of Rubbery Materials, Rapra, Shrewsbury, 2001.
[6] M. Schneider, L. Gasper, D.E. Demco, B. Blümich, Residual dipolar couplings by ^{1}H dipolar encoded longitudinal magnetization, double- and triple-quantum nuclear magnetic resonance in cross-linked elastomers, J. Chem. Phys. 111 (1999) 402–415.
[7] R. Fechete, D.E. Demco, B. Blümich, Chain orientation and slow dynamics in elastomers by mixed magic-Hahn echo decay, J. Chem. Phys. 118 (2003) 2411–2421.
[8] R. Fechete, D.E. Demco, B. Blümich, Segmental anisotropy in strained elastomers by ^{1}H NMR of multipolar spin states, Macromolecules 35 (2002) 6083–6085.
[9] Y. Sharf, U. Eliav, H. Shinar, G. Navon, Detection of anisotropy in cartilage using ^{2}H double-quantum-filtered NMR spectroscopy, J. Magn. Reson. B 107 (1995) 60–67.
[10] H. Shinar, Y. Seo, G. Navon, Discrimination between the different compartments in sciatic nerve by ^{2}H double-quantum-filtered NMR, J. Magn. Reson. 129 (1997) 98–104.
[11] Y. Sharf, S. Akselrod, G. Navon, Measurement of strain exerted on blood vessel walls by double-quantum-filtered ^{2}H NMR, Magn. Reson. Med. 37 (1997) 69–75.
[12] L. Tsoref, H. Shinar, G. Navon, Observation of a ^{1}H double quantum filtered signal of water in biological tissues, Magn. Reson. Med. 39 (1998) 7–11.
[13] K. Ikoma, H. Takamiya, Y. Kusaka, Y. Seo, ^{1}H double-quantum filtered MR imaging of joints tissues: bound water specific images of tendons, ligaments and cartilage, Magn. Reson. Imag. 19 (2001) 1287–1296.
[14] R. Graf, D.E. Demco, S. Hafner, H.W. Spiess, Selective residual dipolar couplings in cross-linked elastomers by ^{1}H double-quantum NMR spectroscopy, Solid State Nucl. Magn. Reson. 12 (1998) 139–152.
[15] B. Blümich, NMR Imaging of Materials, Clarendon Press, Oxford, 2000.
[16] M. Schneider, D.E. Demco, B. Blümich, ^{1}H NMR imaging of residual dipolar couplings in cross-linked elastomers: dipolar-encoded longitudinal magnetization, double-quantum and triple-quantum filters, J. Magn. Reson. 140 (1999) 432–441.
[17] M. Schneider, D.E. Demco, B. Blümich, NMR images of proton residual dipolar coupling from strained elastomers, Macromolecules 34 (2001) 4019–4026.
[18] M. Munowitz, A. Pines, Principles and applications of multiple-quantum NMR, Adv. Chem. Phys. 66 (1987) 1–152.
[19] R.R. Ernst, G. Bodenhausen, A. Wokaun, Principles of Nuclear Magnetic Resonance in One and Two Dimensions, Clarendon Press, Oxford, 1987.
[20] A. Wiesmath, C. Filip, D.E. Demco, B. Blümich, Double-quantum filtered NMR signals in inhomogeneous magnetic fields, J. Magn. Reson. 149 (2001) 258–263.
[21] R. Fechete, D.E. Demco, B. Blümich, U. Eliav, G. Navon, Anisotropy of collagen fiber orientation in sheep tendon by ^{1}H double-quantum-filtered NMR signals, J. Magn. Reson. 162 (2003) 166–175.